JEE Journal of Ecological Engineering

Journal of Ecological Engineering, 2026, 27(3), 435–450
https://doi.org/10.12911/22998993/211694
ISSN 2299–8993, License CC-BY 4.0

Received: 2025.09.25
Accepted: 2025.11.05
Published: 2026.02.01

Sustainable heavy metal removal using coffee husk-derived biochar: Response surface optimization and adsorption mechanisms

Aninda Tifani Puari[1*], Arti Azora[1], Ressa Ade Octaviani[1], Frisca Lora Amalya[1], Rusnam Rusnam[1], Rika Yusniadha[2], Nika Rahma Yanti[1], M.Y. Shukor[3]

[1] Department of Agricultural and Biosystem Engineering, Faculty of Agricultural Technology, Universitas Andalas, West Sumatera
[2] Padang City Environmental Agency, 25171 Padang, West Sumatera
[3] Department of Biochemistry, Faculty of Biotechnology and Biomolecular Sciences, Universiti Putra Malaysia (UPM), 43400 UPM Serdang, Selangor, Malaysia
* Corresponding author's e-mail: anindapuari@ae.unand.ac.id

ABSTRACT

The efficiency of biosorption processes is determined not only by the properties of the biosorbent, but also by the operational conditions under which they are applied. This study emphasized the critical role of operational parameter optimization in enhancing the performance of exhausted coffee husk biochar (ECH-BC) for the removal of Pb (II) and Cu (II) from aqueous solutions. Response surface methodology (RSM) with a Box–Behnken design (BBD) was employed to optimize three key variables: pH, biochar dosage, and contact time. The optimized conditions – pH 6.0, 0.15 g dosage, and 180 minutes for Pb (II), and pH 6.9, 0.05 g dosage, and 135 minutes for Cu(II) – achieved removal efficiencies of 98.1% (32.8 mg/g) for Pb (II) and 96.3% (105.3 mg/g) for Cu (II). Remarkably, these results represent nearly a 100-fold increase in biosorption capacity compared to unoptimized conditions, demonstrating the transformative effect of operational adjustment. Adsorption equilibrium data were better described by the Freundlich isotherm (R^2 = 0.975 for Pb, R^2 = 0.885 for Cu), indicating heterogeneous multilayer adsorption with surface complexation as the dominant mechanism. Characterization by SEM-EDX confirmed the morphological changes and metal deposition on the biochar surface, while FT-IR spectra revealed the involvement of hydroxyl, carbonyl, and carboxylate functional groups in metal binding. Overall, this study established ECH-BC as a cost-effective and sustainable biosorbent, highlighting that the optimization of operational parameters is the key factor in unlocking its maximum potential for heavy metal wastewater treatment.

Keywords: biosorption, contact time, copper, dosage, lead, pH.

INTRODUCTION

The release of heavy metal into water and soil, whether caused by natural events or human activities, poses a significant threat to both the environment and agriculture (Luo et al., 2024; Puari et al., 2025). Lead (Pb) ranks among the top five most harmful heavy metals, and even trace amount of heavy metals in agricultural settings can initiate a process of accumulation through the food chain, ultimately reaching human cells (Alengebawy et al., 2021; McLaughlin et al., 1999). Additionally, while copper (Cu) is an essential nutrient for plants, excessive uptake from the soil can negatively impact plant productivity, leading to decreased crop yields (Fagnano et al., 2020; Hasan et al., 2020). There is a pressing need to propose effective strategies for reducing the concentration of heavy metals in water, considering the cost constraints associated with current technologies (AlJaberi, 2019; Rashid et al., 2021; Satyam and Patra, 2024).

One approach that has been consistently explored for remediating heavy metals from water and soil is the use of adsorption methods (Glob. Assess. Soil Pollut. Rep., 2021; L. Wang et al.,

2022; Zhang et al., 2023). Various potential adsorbents have been identified for capturing Pb and Cu ions, including biochar (Das et al., 2023; Salim et al., 2016; Puari et al., 2024a). The preparation of biochar, including factors like carbonization temperature, duration, and rate, as well as operational conditions such as pH, dosage, and retention time, is specified to the targeted heavy metals and significantly influences the overall cost of the process (Phuengphai et al., 2021; Aninda et al., 2023). Therefore, careful selection of the raw material and parameter settings is crucial to achieving optimal efficiency.

Due to cost limitation, agricultural waste materials, such as exhausted coffee husks (ECH) from infused drink production, have been used as the raw material for biochar (Puari et al., 2022; Puari et al., 2024). The biosorption potential biochar from ECH for heavy metals has been investigated previously, particularly for Pb (Rusnam et al., 2022) and Cu (Puari et al., 2024) ions. However, up to this point, the investigation was primarily focused on optimizing the carbonization process for Pb and Cu ions (Puari et al., 2024; Rusnam et al., 2022). To expedite the use of ECH-BC produced under optimal carbonization conditions, it is important to apply the best operational conditions during the biosorption process (Puari et al., 2024). The previous studies have exposed that different biomass would result in different operational parameter during biosorption process (Ahmed et al., 2021; Puari et al., 2024; Semerjian, 2018). Moreover, the specific targeted heavy metal ion as the pollutant in the water would also result in different specific operational parameter for the specific biomass (Batool et al., 2023). Researchers have turned to dynamic optimization tools like response surface methodology (RSM) to assess and optimize either the carbonization process (Puari et al., 2024b; Puari et al., 2024; Zhou et al., 2019) or the operational conditions of the biosorbent (Parmar et al., 2020; Puari et al., 2024). The relationship between experimental results and model-predicted outcomes can be analyzed using RSM-based statistical tools like the Box-Behnken design (BBD) (Bezerra et al., 2008; Korondi et al., 2021). The primary goal of this study was to predict the capacity of lead and copper removal from aqueous solutions in a batch study using BBD within an RSM-based model. The optimal biosorption capacity was determined based on pH, ECH biochar dosage, and retention time. The adsorption mechanisms of Pb and Cu ions onto ECH biochar were also discussed in terms of isotherms and kinetic rate constants. Additionally, the data obtained through BBD were statistically evaluated using mean square error and probability values to assess data fitness. The effectiveness of heavy metal ion removal from aqueous solutions was examined by analyzing the biochar samples before and after biosorption using SEM-EDX, FT-IR, and XRD techniques.

MATERIAL AND METHODS

Materials and chemicals

Exhausted coffee husk (ECH) as the main precursor of biochar was collected from AGAVI, West Java, Indonesia. Biochar was prepared according to the previous experimental research (Puari et al., 2024; Rusnam et al., 2022). Meanwhile, $Pb(NO_3)_2$ (1000 mg/L) and $Cu(NO_3)_2$ (1000 mg/L) as standard solutions of lead (Pb) and copper (Cu), were underwent further dilution with distilled water. Sodium hydroxide (NaOH) and chloride acid (HCl) (37%) were used for pH adjustment during biosorption experiments. All of the chemicals were purchased from the local distributor of Merck in Indonesia.

Single factor experiment (SFE)

The center values of all operational parameters, namely pH (4–9), time (30–180 minutes), and dosage (0.05–0.25 g) were defined through the single factor experiment, prior to determining the range code of BBD. The experiment was conducted by varying each of the parameter in a certain range. For Pb, the SFE were applied for all three parameters, while for Cu only for pH. The range code of the other two parameters of Cu were based on the Pb. While one parameter was varied, the others were constant, as presented in Table 1.

The initial concentration of the heavy metal solution was 25 mg/L and was placed inside 250 ml Erlenmeyer flask. ECH BC was added into the solution according to the designed dosage and the initial pH was measured prior to adjusting the desired solution pH. Then, 0.1 M NaOH and HCL were used to set the solution pH, and pH measurement was conducted using a pH meter (Mettler Toledo F20). After the pH was set, the solution was agitated during the experiment using an orbital shaker (SK-0330 PRO NESCO Official),

Table 1. Experimental matrix of single factor experiment (SFE) to define center values of Pb and Cu

Parameter	Pb			Cu		
	pH	Time (minutes)	Dosage	pH	Time (minutes)	Dosage
pH	4	60	0.2	4	60	0.1
	5			5		
	6			6		
	7			7		
	8			8		
	9			9		
Dosage	5	60	0.05			
			0.1			
			0.15			
			0.2			
			0.25			
Biosorption time	5	30	0.1			
		60				
		90				
		120				
		150				
		180				

until the reaching the allocated time. Afterward, the solution was filtered using the filter paper to separate the solution and the adsorbent. The concentration of the heavy metal in the solution before and after the experiment was measured using an atomic absorption spectrophotometer (AAS) (AA-6880, Shimadzu, Japan), following the previous technique by (Puari et al., 2022; Puari et al., 2024). The center value was chosen by evaluating the removal efficiency (RE) and the capacity (q_t), which were calculated by using the Equations 1 and 2 (Puariet al., 2024), as follows:

$$RE\ (\%) = \frac{(C_{initial} - C_{final})}{C_{initial}} \times 100\% \quad (1)$$

$$q_t\ \left(\frac{mg}{g}\right) = \frac{(C_{initial} - C_{final})}{dosage} \times Volume \quad (2)$$

where: $C_{initial}$ is the heavy metal concentration before the experiment and C_{final} is the concentration after the experiment. The dosage of biochar was in g and the volume of the solution was in mL.

Biosorption with Box-Bhenken design

Biosorption studies of ECH were carried out using response surface methodology (RSM) using Design Expert software (version 13) (StartEase) to determine the effect of different operating parameters on removal of each targeted heavy metal. The center code (Table 2) of time and dosage were similar for both heavy metals, while for pH was different, which 5 for Pb and 6 for Cu. BBD was underwent seventeen experiments, each for Pb (Table 3) and Cu (Table 4), and was set based on three level of three parameters-factor. The experimental designs were carried out in batch technique using a 250 mL Erlenmeyer flask. An appropriate amount of ECH BC as adsorbent according to the experimental design was added into the flask with 100 mL of synthetic heavy metal of Pb (50 mg/L of lead nitrate) and Cu (50 mg/L of copper nitrate) solutions. The biosorption was carried out following the single factor experiment, as well as the calculation of the actual RE values.

Model validation

The model for the optimum conditions of Pb and Cu were obtained separately and validated through ANOVA analysis, with 95% confidence level ($\alpha = 0.05$) used to determine significance. The optimum conditions of pH, dosage, and contact time for ECH-BC biosorption for Pb (II) and Cu (II) were validated by conducting biosorption experiment under the conditions, with similar initial concentration of Pb (II) and Cu (II) of 50 mg/L.

Table 2. Coded levels of Box-Bhenken design (BBD) of three operational parameters variables for Pb and Cu

Variables	Symbol	Pb			Cu		
		Coded levels					
		-1	0	1	-1	0	1
pH	A	4	5	6	5	6	7
Dosage (g)	B	0.05	0.1	0.15	0.05	0.1	0.15
Biosorption time (minutes)	C	60	120	180	60	120	180

Table 3. Box-Bhenken design for $Pb^{2+}$with predicted and actual values of RE from experiments

Run	Coded values			Actual values			RE (%) Actual values Pb^{2+}	RE (%) Predicted values
	A	B	C	A	B	C		
1	0	1	1	5	0.15	180	74.36 ± 1.07	74.36
2	0	0	0	5	0.1	120	70.19 ± 0.32	68.45
3	-1	1	0	4	0.15	120	55.95 ± 3.63	55.95
4	-1	0	1	4	0.1	180	51.28 ± 2.54	51.28
5	0	0	0	5	0.1	120	70.65 ± 1.38	68.45
6	0	-1	-1	5	0.05	60	33.06 ± 0.98	33.06
7	-1	0	-1	4	0.1	60	32.54 ± 2.16	32.54
8	1	-1	0	6	0.05	120	98.77 ± 0.09	98.77
9	0	-1	1	5	0.05	180	39.87 ± 1.09	39.87
10	0	0	0	5	0.1	120	66.33 ± 0.23	68.45
11	0	1	-1	5	0.15	60	65.25 ± 1.43	65.25
12	1	1	0	6	0.15	120	98.89 ± 0.07	98.89
13	1	0	-1	6	0.1	60	99.18 ± 0.00	99.18
14	1	0	1	6	0.1	180	98.58 ± 0.09	98.58
15	-1	-1	0	4	0.05	120	43.58 ± 5.41	43.58
16	0	0	0	5	0.1	120	69.97 ± 0.14	68.45
17	0	0	0	5	0.1	120	65.10 ± 5.94	68.45

RE was calculated and the percentage error was determined to confirm the model validation.

Isotherm

The adsorption isotherms of ECH-BC on Pb and Cu were studied to provide the information related to the affinity and equilibrium relationship between the adsorbent (ECH-BC) and adsorbate (Pb and Cu) or the value of the adsorbent capacity. In this study, lead and copper ions adsorption on the ECH-BC surface was studied through Langmuir and Freundlich isotherm models. ECH-BC was under went biosorption in 100 mL of Cu (II) and Pb (II) solutions separately, with a varied concentration in a range of 4–18 mg/L. Biosorption experiments were conducted under the optimum condition of pH and contact time.

Langmuir model assumes a finite number of active sites are homogeneously arranged on the surface and energetically equivalent. The equation of Langmuir isotherm was described by Equation 3, while linearization was expressed by Equation 4. Furthermore, the dimensionless separation (RL) was calculated using Equation 5 to characterize the adsorption, as described previously (Ayalew and Aragaw, 2020).

$$\frac{1}{Q_e} = \frac{1}{Q_m} + \frac{1}{kl\ Q_m CE} \tag{3}$$

$$\frac{C_e}{Q_e} = \frac{C_e}{Q_m} + \frac{1}{klQ_m} \tag{4}$$

$$R_L = \frac{1}{1+bC_i} \tag{5}$$

where: *qe* and *qm* were the equilibrium and maximum adsorption capacity (mg/g), respectively; *KL*, the Langmuir adsorption constant (L/mg) and Ce, the adsorbate concentration in the equilibrium (mg/L).

Meanwhile, Freundlich isotherm models were analyzed to obtain characteristic of adsorbent with different affinities or adsorption energies of the active sites. While Langmuir is assumed monolayer adsorption, Freundlich can be assumed multilayer. The linear of isotherm model was expressed in Equation 5 following the previous study (Ayalew and Aragaw, 2020).

$$\log qe = \log kf + \left(\frac{1}{n}\right) \times \log Ce \qquad (6)$$

where: k_f was Freundlich adsorption constant, and n described the affinity between adsorbent and adsorbate and intensity of the adsorbent. The value of n was characterized into three range; if the value n <1, adsorption is unfavorable. On the contrary, when n>1, the adsorption onto the adsorbent surface is favorable. It is noteworthy, high value of n reflects strong sorption intensity.

Biochar characterization techniques

Several experimental instruments were used to characterize the materials before and after biosorption at the optimum condition. The morphological surface of adsorbent and the elemental composition on it was examined using Scanning Electron Microscope with energy dispersive X-Ray (SEM-EDX) (SEM-EDX JEOL JSM-6510 LA, Tokyo Japan). Meanwhile, identification of surface functional groups was conducted by an IRTracer-100 Fourier Transform Infrared Spectrophotometer (FTIR) (Shimadzu, Japan).

RESULTS AND DISCUSSION

Center value of single factor experiment

The center values for each parameter in the single factor experiment (SFE) were established based on the biosorption performance of each factor. In this study, the effect of pH factor on the biosorption of Pb (II) and Cu (II) was evaluated separately for each metal, whereas the effect of biochar dosage and contact time were investigated only for Pb (II), with the resulting center values also applied to Cu (II).

Figure 1 presented the biosorption performance of ECH biochar at the varying pH values (4–8). An increase in both removal efficiency (RE) and biosorption capacity (q_t) was observed when pH increased from 4 to 5 for both metals (Figures 1a and 1b). This increase was more pronounced for Cu (II), with Re improving from 26% to 68%, compared to Pb (II), which increased from 94% to 99.5%. Beyond pH 5, Re for Pb(II) plateaued, indicating that optimal removal was already achieved. In contrast, Cu (II) continued to show a

Table 4. Box-Bhenken design for Cu^{2+} with predicted and actual values of RE from experiments

Run	Coded values			Actual values			RE (%) Actual values Cu^{2+}	RE (%) Predicted values
	A	B	C	A	B	C		
1	0	1	1	6	0.15	180	98.83 ± 0.11	99.37
2	0	0	0	6	0.01	120	66.78 ± 0.47	67.07
3	-1	1	0	5	0.15	120	47.06 ± 0.27	47.43
4	-1	0	1	5	0.1	180	50.08 ± 0.66	49.17
5	0	0	0	6	0.1	120	70.74 ± 0.05	67.07
6	0	-1	-1	6	0.05	60	89.14 ± 0.14	88.60
7	-1	0	-1	5	0.1	60	49.19 ± 0.25	43.19
8	1	-1	0	7	0.05	120	99.60 ± 0.04	99.23
9	0	-1	1	6	0.05	180	98.71 ± 0.06	93.08
10	0	0	0	6	0.01	120	71.34 ± 0.20	67.07
11	0	1	-1	6	0.15	60	86.93 ± 0.46	92.56
12	1	1	0	7	0.15	120	99.75 ± 0.01	93.21
13	1	0	-1	7	0.1	180	99.55 ± 0.01	100.46
14	1	0	1	7	0.1	180	99.78 ± 0.07	105.78
15	-1	-1	0	5	0.05	120	24.61 ± 1.58	31.15
16	0	0	0	6	0.01	120	64.91 ± 0.07	67.07
17	0	0	0	6	0.01	120	61.57 ± 0.40	67.07

significant increase in both RE (from 68% to 98%) and q_t (from 16.4 to 23.7 mg/g) when the pH increased from 5 to 6. These results confirm that the optimal pH varies with the type of metal ion: pH 5 for Pb (II) and pH 6 or Cu (II). This trend is consistent with the findings from previous studies by AlOthman et al. (2016), Ahmad et al. (2022), and Wang et al. (2025), which also reported optimal biosorption performance within a pH range of 5–6 for both metals. On the basis of these findings, a pH of 5 was selected as the central value for Pb(II) in the BBD experiment, while pH 6 was chosen for Cu (II). The biosorption of Pb and Cu under biochar from different biomass, resulted the optimum pH in the range of 5–6 for both metals. Hence, pH of 5 was defined as the center value for BBD experiment of Pb, while pH of 6 for Cu.

For the analysis of biochar dosage (Figure 1c) and contact time (Figure 1d), the solution of pH was fixed at 5. As it is shown in Figure 1c, an increase in biochar dosage generally enhanced the removal efficiency. Specifically, increasing the dosage from 0.05 g to 0.1 g (in 250 mL of Pb(II) solution with a 60-minute contact time) improved RE from 77.6% to 87.5%. A further increase to 0.15 g raised RE to 96.6%. However, RE gains diminished beyond this point, with only a 2.7% increase (up to 99.2%) at 0.2 g dosage. Simultaneously, the biosorption capacity (q_t) showed a decreasing trend, dropping from 38.5 mg/g at 0.05 g to 21.7 mg/g at 0.1 g, and continuing to decline to 16 mg/g and 12.3 mg/g at higher dosage. Although the highest q_t was observed at the lowest dosage (0.05 g), RE was still limited to 77.6%. Therefore, a dosage of 0.01 g was selected as the center value for both Pb (II) and Cu(II).

The third factor studied was contact time, varied in a range of 30 to 180 minutes. Previous studies have reported different optimal times for metal biosorption, 180 minutes (AlOthman et al., 2016; Ahmadi et al., 2022) and 30 minutes (Semerjian, 2018). In this study, RE increased progressively with longer contact time (Figure 1d). RE reached 80% at 30 minutes, and further increased to 92% at 120 minutes. Minor improvements were observed with longer durations, reaching 93% at 150 minutes and 96% at 180 minutes. On the basis of these observations, 120 minutes was selected as the center value for contact time in the BBD experiment.

Analysis of RSM-BBD

Tables 3 and 4 presented the RE results for Pb (II) and Cu (II), respectively, under various

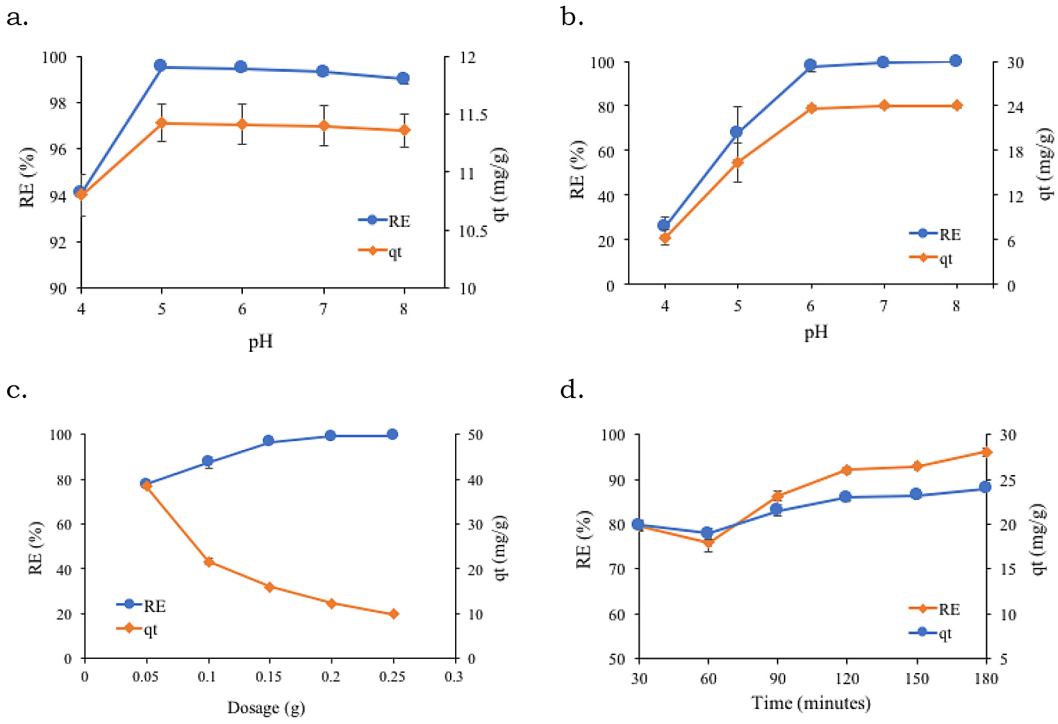

Figure 1. The biosorption performances, RE (% and q_t (mg/g), under various a) pH on Pb, b) pH on Cu, c) dosage on Pb, and d) time on Pb

experimental conditions following the BBD for a statistical optimization. Columns 5,6, and 7 of each table listed the actual values of the operating parameters; pH, dosage and contact time. The experimental RE outcomes for the ions of both metals were varied according to the design matrix. Although the magnitude of RE differed between Pb (II) and Cu (II), the highest RE values for both metals were observed in the same experimental runs. Specifically, as shown in Tables 3 and 4, RE values exceeding 95% were recorded in runs 8, 12 13, and 14. In all of these runs, the pH setting was at level 1 of the matrix scale, corresponding to pH 6 for Pb (II) and pH 7 for Cu (II). This suggests that despite the difference in optimum pH for each metal, there is a consistent pattern in the design matrix where similar combinations of parameters yield high RE for both metals.

Regression analysis using both quadratic and cubic models were carried out based on the 17 experimental data points, and the analysis of variance (ANOVA) was used to evaluate the statistical significance of the model and parameters. A 95% confidence level ($\alpha = 0.05$) was used to determine significance. As presented in Table 5, the quadratic model for Pb (II) biosorption was defined statistically significant, with p value of 0.001. However, the lack-of-fit p-value of quadratic model was 0.0068 ($p < 0.05$), indicating a significant lack-of-fit. The lack of fit test evaluates the model's failure to represent the system in the unexplored portions of the design space; therefore, a non-significant result is desirable to confirm model validity. The significant lack-of fit of the quadratic model suggests that the model does not adequately describe the biosorption behavior (Puari et al., 2024a).

Aa a result, cubic regression model was applied, and the corresponding ANOVA results were shown in Table 6. The cubic model yielded a statistically acceptable fit based on the obtained p-values. Furthermore, a comparison of the signal-to-noise ratio (SNR), coefficient of determination (R^2) and adjusted R^2 for both models- as presented in Table 7-demonstrated that the cubic model outperformed the quadratic model. Both models exhibited SNR values higher than 4, which is considered desirable according to Haaland (2020). However, the higher SNR of the cubic model indicates it provides a stronger and more reliable response signal for the Pb (II) biosorption process (Puari et al., 2024a). In addition, the R^2 and adjusted R^2 values for the cubic model were closer to 1, further supporting its superior fit. On the basis of these findings, the cubic regression model was determined to be more suitable for predicting and optimizing the Pb (II) biosorption performance in this study, and the model equation was expressed in Equation 7, where A, B and C are coded levels for pH, dosage and time, respectively.

Table 5. The quadratic resgression model of ANOVA for removal efficiency of Pb by ECH-biochar

Source	Sum of squares	df	Mean square	F-value	p-value	
Removal efficiency (%)						
Model	7719.36	9	857.71	14.13	0.0010	significant
A-pH	5621.71	1	5621.71	92.63	< 0.0001	
B-Dosage	783.49	1	783.49	12.91	0.0088	
C-Time	145.01	1	145.01	2.39	0.1661	
AB	37.52	1	37.52	0.6182	0.4575	
AC	93.51	1	93.51	1.54	0.2545	
BC	1.32	1	1.32	0.0218	0.8868	
A^2	562.16	1	562.16	9.26	0.0188	
B^2	137.05	1	137.05	2.26	0.1766	
C^2	388.67	1	388.67	6.40	0.0392	
Residual	424.82	7	60.69			
Lack of fit	398.93	3	132.98	20.54	0.0068	significant
Pure error	25.89	4	6.47			
Cor total	8144.19	16				

Table 6. The cubic resgression model of ANOVA for removal efficiency of Pb by ECH-biochar

Source	Sum of squares	df	Mean square	F-value	p-value	
Removal efficiency (%)						
Model	8118.29	12	676.52	104.50	0.0002	significant
A-pH	3245.58	1	3245.58	501.35	< 0.0001	
B-Dosage	1111.56	1	1111.56	171.70	0.0002	
C-Time	63.36	1	63.36	9.79	0.0352	
AB	37.52	1	37.52	5.80	0.0738	
AC	93.51	1	93.51	14.44	0.0191	
BC	1.32	1	1.32	0.2043	0.6747	
A^2	562.16	1	562.16	86.84	0.0007	
B^2	137.05	1	137.05	21.17	0.0100	
C^2	388.67	1	388.67	60.04	0.0015	
ABC	0.0000	0				
A^2B	367.07	1	367.07	56.70	0.0017	
A^2C	0.6161	1	0.6161	0.0952	0.7731	
AB^2	31.24	1	31.24	4.83	0.0930	
AC^2	0.0000	0				
B^2C	0.0000	0				
BC^2	0.0000	0				
A^3	0.0000	0				
B^3	0.0000	0				
C^3	0.0000	0				
Pure Error	25.89	4	6.47			
Cor Total	8144.19	16				

$$Y_{RE(\%)} = 68.45 + 28.48A + 16.67B + \\ + 3.98C - 3.06AB - 4.84AC + 0.5750BC + \\ + 11.55A^2 - 5.71B^2 - 9.61C^2 - \\ - 13.55A^2B + 0.5550A^2C - 3.95AB^2 \quad (7)$$

In the case of Cu (II) biosorption, the quadratic regression model produced a statistically significant p-value, along with a non-significant lack-of-fit value, as shown in Table 8. These results indicated that the model is a good fit for the experimental data. The model exhibited a signal-to-noise ratio (SNR) of 15.12, which is well above the minimum threshold (Haaland, 2020), considered desirable of reliable model interpretation. Additionally, the model achieved a coefficient determination higher (R^2) and adjusted R^2 than 0.9, with 0.9674 and 0.9255, respectively -both indicating strong predictive accuracy for the quadratic model. These metrics support the conclusion that the quadratic response surface model is well-suited for describing Cu (II) biosorption by ECH biochar under the three process variables considered (pH, dosage, and time). A similar trend on biosorption of Cu (II) ions using other biomass, was reported in a study by Fawzy et al. (2022), where the quadratic model also valid for the optimization and prediction in heavy metal biosorption process. The model equation for the prediction of Cu biosorption by ECH was exhibited in the Equation 8. A was expressed for pH, while B and C were for dosage and time, respectively.

$$Y_{RE(\%)} = 67.07 + 28.47\,A + 2.56\,B + \\ + 2.82\,C - 5.57\,AB - 0.165\,AC + \\ +0.5825BC - 9.03\,A^2 + 9.72\,B^2 + 16.61\,C^2 \quad (8)$$

3D surfaces plots and model validation

3D surface plots

The 3D surfaces plots depicting of the RE of Pb (II) and Cu (II) were presented in Figure 2. These plots illustrated the interactive effects between pairs of operating parameters and their impact on the response variable, providing valuable insights into the combined influence of experimental conditions on RE as well as the optimal

Table 7. The values of quadratic and cubic regression models

Regression model	R^2	Adjusted R^2	SNR
Quadratic	0.9478	0.8808	12.1920
Cubic	0.9968	0.9873	29.9510

Table 8. The quadratic regression model of ANOVA for removal efficiency of Cu by ECH-biochar

Source	Sum of squares	df	Mean square	F-value	p-value	
Removal Efficiency (%)						
Model	78604.24	9	956.03	23.07	0.002	significant
A-pH	6483.19	1	6483.19	156.48	< 0.0001	
B-Dosage	52.58	1	52.58	1.27	0.2971	
C-Time	63.79	1	63.79	1.54	0.2546	
AB	124.32	1	124.32	3.00	0.1268	
AC	0.1089	1	0.1089	0.0026	0.9605	
BC	1.36	1	1.36	0.0328	0.8615	
A^2	343.54	1	343.54	8.29	0.0237	
B^2	397.78	1	397.78	9.60	0.0174	
C^2	1162.32	1	1162.32	28.50	0.0011	
Residual	290.02	7	41.43			
Lack of fit	223.32	3	74.44	4.46	0.0912	not significant
Pure error	66.70	4	16.68			
Cor total	8894.26	16				

Note: *R^2 = 0.9674, adjusted R^2=0.9255,SNR = 15.1166.

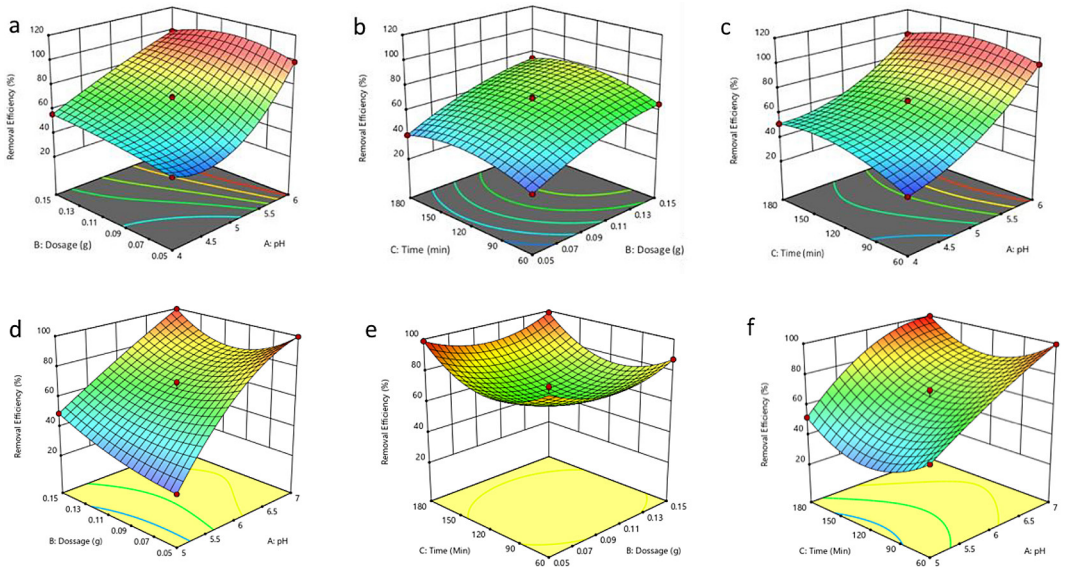

Figure 2. 3D surface plots of ECH biochar on Pb RE through interaction of two parameters a) dosage and pH, b) time and dosage, c) time and pH; and on Cu through interaction of two parameters d) dosage and pH, e) time and dosage, f) time and pH

parameter configurations. For both Pb (II) (Figures 2a-c) and Cu (II) (Figures 2d-f), the initial pH was shown to significantly influence the interaction patterns and resulting removal performance.

Among the interactions, the combination of pH and contact time yielded the highest RE values for both metal ions. This finding aligns with the ANOVA results for Pb (II) biosorption (Table

6), where the interaction between pH and time was the only statistically significant two-factor interaction. In general, increasing the pH led to an enhancement in RE across all factor combinations. This trend is consistent with the explanation by Bayik et al. (Haaland, 2020), who noted that at low (acidic) pH levels, H^+ ions and metal cations compete for the active binding sites on the biosorbent surface. Moreover, under acidic conditions, the total surface charge of the biosorbent becomes less negative, thereby reducing its capacity to attract positively charged metal ions (Jena et al., 2022; Yang and Cui, 2013). Consequently, a higher pH favors metal ion uptake by reducing such electrostatic competition.

Model validation

Figure 2 demonstrated the interaction between pH and contact time, as well as pH and biochar dosage resulted in RE approaching 100%. These results confirm that the biosorption of Pb (II) and Cu (II) using ECH-biochar (ECH-BC) was conducted under near-optimal operational conditions, supporting the validity of the model predictions. The optimal values for the three operational parameters-pH, dosage, and contact time-were determined using Design-expert software. The optimized parameter combinations for Pb (II) and Cu (II) biosorption were presented in Table 9.

The optimal pH values for ECH-BC biosorption of Pb (II) and Cu (II) were found to be within the slightly acidic to neutral range (6.0–6.9), a condition favorable for minimizing competition from H^+ ions and enhancing metal ion uptake. The model-predicted outcomes were validated by performing biosorption experiments under the proposed optimal conditions, with the experimental results were also shown in Table 9.

Notably, achieving 98–99% removal efficiency for both metal ions required different biochar dosages, where the dosage for Pb (II) removal was approximately three times greater than for Cu (II). This resulted in a lower biosorption capacity of ECH-BC in Pb (II) compared to Cu (II). The observation suggests a higher affinity or more efficient binding behavior of ECH-BC toward Cu (II) under similar conditions. Furthermore, the biosorption of Cu (II) reached equilibrium more rapidly than that of Pb (II), indicating a faster kinetic response. Similar findings were also reported by Ahmadi et al. (2022), where Pb (II) exhibited a lower biosorption capacity than Cu (II), using melon-peel biosorbent under identical contact times. In all cases, the experimental results closely matched the model predictions, with a percent error of less than 10%, confirming the reliability and predictive accuracy of the develop model of optimizing biosorption conditions of Pb (II) and Cu (II) using ECH-BC

Isotherm model

To investigate the biosorption behavior of ECH-BC toward Pb (II) and Cu (II), adsorption isotherm analysis was conducted using both Langmuir and Freundlich isotherm models. The equilibrium data for the biosorption Pb (II) and Cu (II) onto ECH-BC were fitted to these models, and the corresponding plots were presented in Figures 3a-d. The derived parameters and correlation coefficients were summarized in Table 10.

From the data, it was observed that the dimensionless separation factor (RL) values were 0.076 for both Pb^{2+} and Cu^{2+} in the Langmuir model, indicating favorable adsorption ($0 < RL < 1$). The maximum monolayer adsorption capacity (q_m) obtained from the Langmuir model was higher for Pb^{2+} (312 mg/g) than for Cu^{2+} (196.1 mg/g). The outcomes of Pb and Cu removal from this study are promising compared to other previous studies as presented in Table 11. The obtained results were also significantly higher compared to the previous study of ECH biochar on the both heavy metal, which increased by nine times higher after the optimization of the operational parameters. However, the low correlation coefficient (R^2) (R^2 = 0.748

Table 9. Predicted optimum condition of operational parameters (pH, biochar dosage, and contact time)

Ions	Optimum conditions			Response values	Predicted values	Experimental value			
	pH	Dosage (g)	Time (minutes)			1	2	3	Average
Pb^{2+}	6	0.15	180	RE (%)	98.02	98.0	98.3	98.0	98.1 ± 0.2
				qt (mg/g)	30.28	32.9	32.8	32.7	32.8 ± 0.1
Cu^{2+}	6.9	0.05	134.92	RE (%)	99.77	96.3	96.2	96.3	96.3 ± 0.1
				qt (mg/g)	114.42	105.3	105.3	105.2	105.3 ± 0.06

Table 10. Derived parameters and correlation coefficient of isotherm models for ECH-BC on Pb^{2+} and Cu^{2+}

Elements	Langmuir isotherm				Freudlich isotherm		
	q_m (mg/g)	K_L (L/mg)	R_L	R^2	K_F (mg/g(mg/L$^{-1/n}$))	n	R^2
Pb^{2+}	312.5	0.762	0.076	0.748	132.71	1.55	0.975
Cu^{2+}	196.1	0.761	0.076	0.705	87.78	1.42	0.885

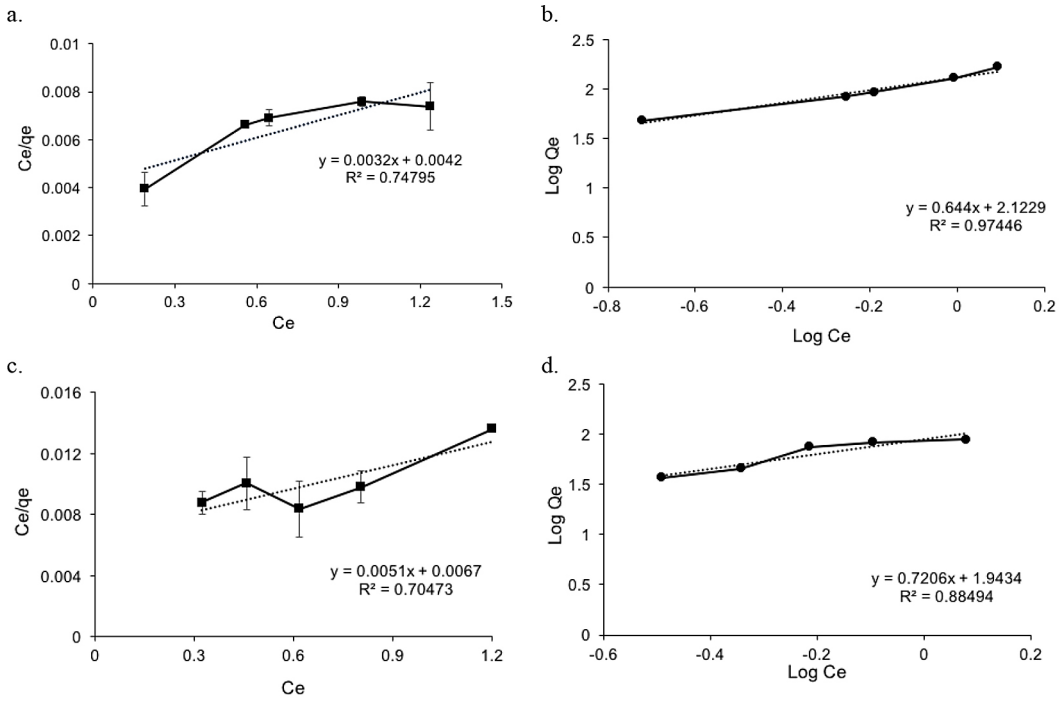

Figure 3. a) Langmuir isotherm and b) Freudlich isotherm plots of Pb (II); c) Langmuir isotherm, b) Freundlich isotherm plots of Cu (II)

for Pb^{2+} and R^2 = 0.705 Cu^{2+}) suggested that the Langmuir model did not adequately describe the biosorption behavior. In contrast, the Freundlich model showed a better fit to the experimental data, with higher correlation coefficients - R^2= 0.975 for Pb^{2+} and R^2 = 0.885 for Cu^{2+}. This indicates that the biosorption process followed a heterogeneous surface adsorption mechanism and supports the occurrence of adsorption complexation reactions rather than monolayer adsorption. These findings were consistent with previous studies, such as the biosorption of Pb (II) and Cu (II) onto pine sawdust (Semerjian, 2018) and green straw-derived biochar (TB) (Wang et al., 2025).

Characterization

SEM-EDX

Figure 4 a-c presented the morphological and elemental characteristics of ECH biochar (ECH-BC) before and after underwent biosorption of Pb^{2+} and Cu^{2+} from SEM-EDX investigation. As it is shown in Figure 4a, ECH-BC exhibited a high density of pores and well-structured surface with open macropores and relatively smooth texture, indicating high surface accessibility for metal ion interaction.

Meanwhile, after Cu (II) biosorption (Figure b), the surface became rougher and irregular, with visible particulate deposits suggesting Cu accumulation on the surface. The EDX analysis confirmed the presence of Cu on the surface with an 5.44%, increased from 0.61% before the biosorption, indicating a successful biosorption. Similarly, the biochar after Pb (II) exposure (Figure c) displayed more compact and agglomerated surface features with diminished pore visibility, likely due to Pb precipitation or strong surface binding. The EDX data supported this observation, showing a Pb presence with atomic percentage of 4.57%. In both cases, the appearance of metal peaks and a reduction in carbon percentage

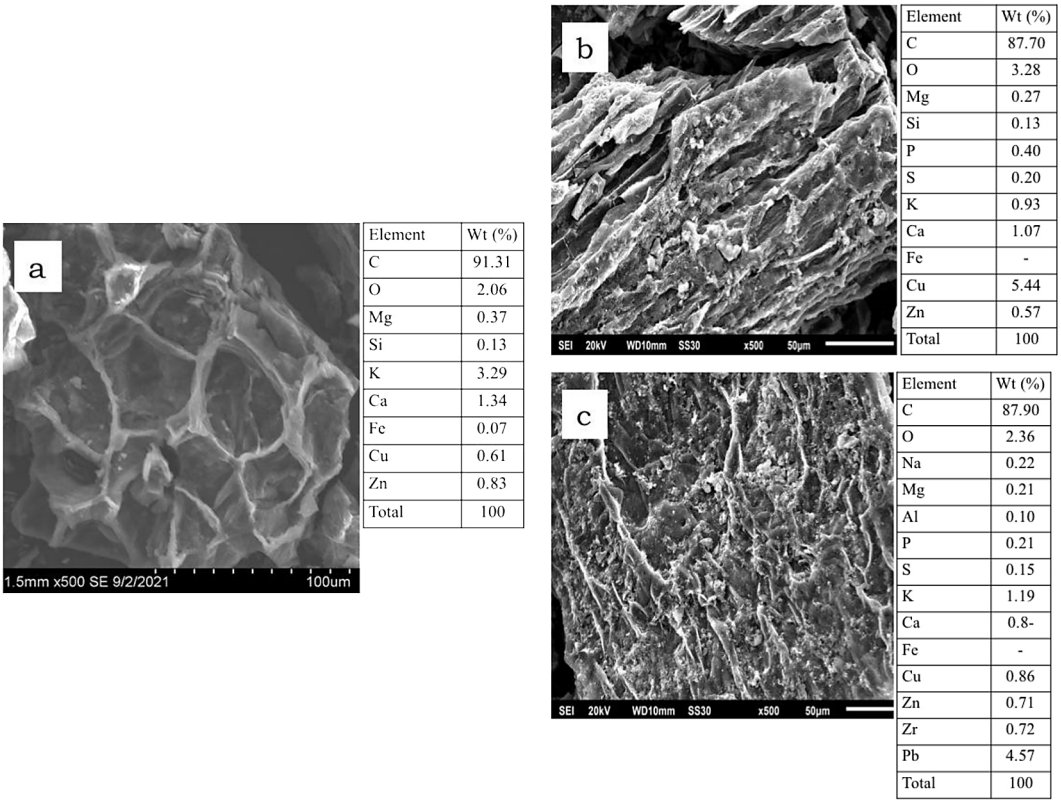

Element	Wt (%)
C	91.31
O	2.06
Mg	0.37
Si	0.13
K	3.29
Ca	1.34
Fe	0.07
Cu	0.61
Zn	0.83
Total	100

Element	Wt (%)
C	87.70
O	3.28
Mg	0.27
Si	0.13
P	0.40
S	0.20
K	0.93
Ca	1.07
Fe	-
Cu	5.44
Zn	0.57
Total	100

Element	Wt (%)
C	87.90
O	2.36
Na	0.22
Mg	0.21
Al	0.10
P	0.21
S	0.15
K	1.19
Ca	0.8-
Fe	-
Cu	0.86
Zn	0.71
Zr	0.72
Pb	4.57
Total	100

Figure 4. SEM images and EDX elemental analysis of ECH-biochar a) before biosorption, b) after biosorption of Cu^{2+}, c) after biosorption of Pb^{2+}

suggest that Cu and Pb ions were immobilized via mechanisms such as surface complexation with oxygen-containing functional groups, electrostatic attraction, and ion exchange. These findings were in line with recent studies of Dey et al. (2022) and Fawzy et al. (2022), where the ion exchange as a mechanism of biosorption were detected through SEM-EDX results.

FTIR

The FTIR spectra of biochar before and after underwent biosorptions of Pb (II) and Cu (II) were presented in Figure 5. The spectra revealed distinct variations in the intensity and position of characteristic absorption bands, indicating changes in the functional groups involved in metal ion interaction. In the broad spectral region between 3600 and 3200 cm^{-1} (region 1), corresponding to the stretching vibrations of hydroxyl (-OH) and amine (-NH) groups, a noticeable decrease in transmittance was observed after biosorption. It suggests the polar functional groups may participate in hydrogen bonding or surface complexation with the metal ions. Meanwhile, peak band in the range of 3000–2800 cm^{-1} (region 2), typically associated with aliphatic C-H stretching, exhibited minimal change, indicating that these non-polar groups are not significantly involved in the biosorption mechanism. Although the 2500–2200 cm^{-1} region (region 3), often attributed to triple bonds such as C ≡ C or C ≡ N, showed very weak or absent peaks in all samples, the most prominent changes were observed in regions 4 and 5, specifically between 1750–1500 cm^{-1} and 1450–1000 cm^{-1}, respectively. Region 4 included the characteristic vibrations of carbonyl (C=O), aromatic C=C, and amide C-N functional groups, which showed a shift in peak position and a decline in transmittance following metal ion exposure, thereby indicating the interaction of Pb^{2+} and Cu^{2+} with electron-rich sites on the biochar surface. Similarly, the significant decrease in intensity observed in region 5 prior to biosorption, which corresponds to C-O stretching vibrations and carboxylate ($-COO^-$) groups. The finding supports the indication of involvement of oxygenated functional groups in binding the heavy metals ions, as the decrease of carbon percentage in EDX analysis.

Overall, the FTIR spectra provided strong evidence that surface functional groups play a central role in the biosorption process and are responsible or the immobilization of the metal ions

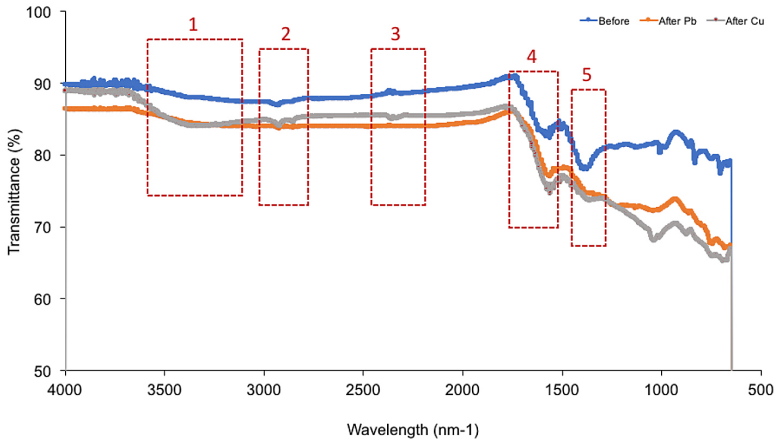

Figure 5. FT-IR spectra of ECH-BC before and after undergoing biosorption of Pb^{2+} and Cu^{2}

Table 11. Comparison of biosorbent capacities from various agricultural wastes

Biosorbent	q_m Pb (mg/g)	q_m Cu (mg/g)	References
Palm kernel shell (PKS)	0.17	-	(Dechapanya and Khamwichit, 2023)
Pine sawdust	13.48	9.59	(Semerjian, 2018)
Mixed-waste activated carbon	122	220	(ALOthman et al., 2016)
Straw biochar	46.98	60.86	(X. Wang et al., 2025)
Limestone mining waste	270.3	73.53	(Fathy et al., 2025)
Water melon seed	44.32	-	(Ahmed et al., 2021)
Melon peel	191.93	77.76	(Ahmadi et al., 2022)
Mango seed	263.4	-	(Q. Wang et al., 2022)
Food waste biochar	245.5	-	(Tian et al., 2023)
Banana peel powder	89.28	5.72	(Mohd Salim et al., 2016)
EKC biochar	-	12.76	(Aninda et al., 2024a)
ECH biochar without optimization	3.3	2.4	(Puari et al., 2024; Rusnam et al., 2022)
This study	312.5	196.1	This study

onto the biochar matrix. These findings were consistent with recent studies of Wang et al. (2025) and Ahmed et al. (2021), which highlighted the involvement of carboxyl and hydroxyl groups in Pb (II) and Cu (II) binding on biochar surfaces.

CONCLUSIONS

Exhausted coffee husk – biochar (ECH-BC) demonstrated high efficiency in the removal of Pb^{2+} and Cu^{2+} from aqueous solutions, under optimized operational conditions determined by response surface methodology. The predictive model for Pb^{2+} followed a cubic model, while that for Cu^{2+} was best described by a quadratic model. The optimum parameters were pH 6.0, 0.15 g dosage, and 180 min for Pb^{2+}, and pH 6.9, 0.05 g dosage, and 134.92 for Cu^{2+}, reflecting a slight difference in pH preference between the two metals. Model predictions closely matched experimental results, achieving 98.1% removal (32.8 mg/g) for Pb and 96.3% removal (105.3 mg/g) for Cu. Adsorption followed the Freundlich model, with higher correlation coefficients – R^2= 0.975 for Pb^{2+} and R^2 = 0.885 for Cu^{2}, indicating heterogeneous surface binding and adsorption-complexation as the dominant mechanism. SEM-EDX and FTIR analyses before and after biosorption confirmed morphological changes and decreased carbon content, consistent with metal ion binding. FTIR spectra indicated reductions in transmittance at peaks associated with C-O stretching and carboxylate ($-COO^-$) groups, confirming the role of oxygen-containing functional groups in metal coordination. These findings highlight ECH-BC as promising, low-cost biosorbent for practical heavy metal wastewater treatment.

Acknowledgement

The Authors wish to acknowledge Mesa Irna Suryani (Central Laboratory, Faculty of Pharmacy) for the fruitful discussion during FTIR analysis.

REFERENCES

1. Ahmadi, H., Hafiz, S. S., Sharifi, H., Rene, N. N., Habibi, S. S., Hussain, S. (2022). Low cost biosorbent (Melon Peel) for effective removal of Cu (II), Cd (II), and Pb (II) ions from aqueous solution. *Case Studies in Chemical and Environmental Engineering*, *6*(August), 100242. https://doi.org/10.1016/j.cscee.2022.100242
2. Ahmed, W., Mehmood, S., Núñez-delgado, A., Ali, S., Qaswar, M., Shakoor, A., Mahmood, M., Chen, D. (2021). Science of the Total Environment Enhanced adsorption of aqueous Pb (II) by modi fi ed biochar produced through pyrolysis of watermelon seeds. *Science of the Total Environment*, *784*, 147136. https://doi.org/10.1016/j.scitotenv.2021.147136
3. Alengebawy, A., Abdelkhalek, S. T., Qureshi, S. R., Wang, M. Q. (2021). Heavy metals and pesticides toxicity in agricultural soil and plants: Ecological risks and human health implications. *Toxics*, *9*(3), 1–34. https://doi.org/10.3390/toxics9030042
4. AlJaberi, F. Y. (2019). Operating cost analysis of a concentric aluminum tubes electrodes electrocoagulation reactor. *Heliyon*, *5*(8), e02307. https://doi.org/10.1016/j.heliyon.2019.e02307
5. AlOthman, Z. A., Habila, M. A., Al-Shalan, N. H., Alfadul, S. M., Ali, R., Rashed, I. G. A., Alfarhan, B. (2016). Adsorptive removal of Cu(II) and Pb(II) onto mixed-waste activated carbon: kinetic, thermodynamic, and competitive studies and application to real wastewater samples. *Arabian Journal of Geosciences*, *9*(4). https://doi.org/10.1007/s12517-016-2350-9
6. Ayalew, A. A., Aragaw, T. A. (2020). Utilization of treated coffee husk as low-cost bio-sorbent for adsorption of methylene blue. *Adsorption Science and Technology*, *38*(5–6), 205–222. https://doi.org/10.1177/0263617420920516
7. Batool, F., Qadir, R., Adeeb, F., Kanwal, S., Abdelrahman, E. A., Noreen, S., Albalawi, B. F. A., Mustaqeem, M., Imtiaz, M., Ditta, A., Gondal, H. Y. (2023). Biosorption potential of arachis hypogaea-derived biochar for Cd and Ni, as evidenced through kinetic, isothermal, and thermodynamics modeling. *ACS Omega*, *8*(43), 40128–40139. https://doi.org/10.1021/acsomega.3c02986
8. Bezerra, M. A., Santelli, R. E., Oliveira, E. P., Villar, L. S., Escaleira, L. A. (2008). Response surface methodology (RSM) as a tool for optimization in analytical chemistry. In *Talanta*. https://doi.org/10.1016/j.talanta.2008.05.019
9. Das, A., Bar, N., Das, S. K. (2023). Adsorptive removal of Pb(II) ion on Arachis hypogaea's shell: Batch experiments, statistical, and GA modeling. *International Journal of Environmental Science and Technology*, *20*(1), 537–550. https://doi.org/10.1007/s13762-021-03842-w
10. Dechapanya, W., Khamwichit, A. (2023). Biosorption of aqueous Pb(II) by H_3PO_4-activated biochar prepared from palm kernel shells (PKS). *Heliyon*, *9*(7), e17250. https://doi.org/10.1016/j.heliyon.2023.e17250
11. Dey, S., Sreenivasulu, A., Veerendra, G. T. N., Phani Manoj, A. V., Haripavan, N. (2022). Synthesis and characterization of mango leaves biosorbents for removal of iron and phosphorous from contaminated water. *Applied Surface Science Advances*, *11*(August). https://doi.org/10.1016/j.apsadv.2022.100292
12. Fagnano, M., Agrelli, D., Pascale, A., Adamo, P., Fiorentino, N., Rocco, C., Pepe, O., Ventorino, V. (2020). Copper accumulation in agricultural soils: Risks for the food chain and soil microbial populations. *Science of The Total Environment*, *734*, 139434. https://doi.org/10.1016/J.SCITOTENV.2020.139434
13. Fathy, A. T., Moneim, M. A., Ahmed, E. A., El-Ayaat, A. M., Dardir, F. M. (2025). Effective removal of heavy metal ions (Pb, Cu, and Cd) from contaminated water by limestone mine wastes. *Scientific Reports*, *15*(1), 1680. https://doi.org/10.1038/s41598-024-82861-2
14. Fawzy, M. A., Al-Yasi, H. M., Galal, T. M., Hamza, R. Z., Abdelkader, T. G., Ali, E. F., Hassan, S. H. A. (2022). Statistical optimization, kinetic, equilibrium isotherm and thermodynamic studies of copper biosorption onto Rosa damascena leaves as a low-cost biosorbent. *Scientific Reports*, *12*(1), 1–19. https://doi.org/10.1038/s41598-022-12233-1
15. Fawzy, M. A., Darwish, H., Alharthi, S., Al-Zaban, M. I., Noureldeen, A., Hassan, S. H. A. (2022). Process optimization and modeling of Cd2+ biosorption onto the free and immobilized *Turbinaria ornata* using Box–Behnken experimental design. *Scientific Reports*, *12*(1), 1–18. https://doi.org/10.1038/s41598-022-07288-z
16. Global assessment of soil pollution: Report. (2021). *Global Assessment of Soil Pollution: Report*. https://doi.org/10.4060/CB4894EN
17. Haaland, P. D. (2020). Experimental design in biotechnology. In *Experimental Design in Biotechnology*. https://doi.org/10.1201/9781003065968
18. Hasan, A. B., Reza, A. H. M. S., Kabir, S., Siddique, M. A. B., Ahsan, M. A., Akbor, M. A. (2020). Accumulation and distribution of heavy metals in soil and food crops around the ship breaking area in southern Bangladesh and associated health risk

assessment. *SN Applied Sciences*, *2*(2), 1–18. https://doi.org/10.1007/s42452-019-1933-y

19. Korondi, P. Z., Marchi, M., Poloni, C. (2021). Response surface methodology. In *Optimization Under Uncertainty with Applications to Aerospace Engineering*. https://doi.org/10.1007/978-3-030-60166-9_12
20. Luo, F., Zhang, F., Zhang, W., Huang, Q., Tang, X. (2024). Distribution, ecological risk, and source identification of heavy metal(loid)s in sediments of a headwater of Beijiang River affected by mining in Southern China. *Toxics*, *12*(2), 1–17. https://doi.org/10.3390/toxics12020117
21. McLaughlin, M. J., Parker, D. R., Clarke, J. M. (1999). Metals and micronutrients - Food safety issues. *Field Crops Research*, *60*(1–2), 143–163. https://doi.org/10.1016/S0378-4290(98)00137-3
22. Mohd Salim, R., Khan Chowdhury, A. J., Rayathulhan, R., Yunus, K., Sarkar, M. Z. I. (2016). Biosorption of Pb and Cu from aqueous solution using banana peel powder. *Desalination and Water Treatment*, *57*(1), 303–314. https://doi.org/10.1080/19443994.2015.1091613
23. Parmar, P., Shukla, A., Goswami, D., Patel, B., Saraf, M. (2020). Optimization of cadmium and lead biosorption onto marine Vibrio alginolyticus PBR1 employing a Box-Behnken design. *Chemical Engineering Journal Advances*, *4*(July). https://doi.org/10.1016/j.ceja.2020.100043
24. Phuengphai, P., Singjanusong, T., Kheangkhun, N., Wattanakornsiri, A. (2021). Removal of copper(II) from aqueous solution using chemically modified fruit peels as efficient low-cost biosorbents. *Water Science and Engineering*, *14*(4), 286–294. https://doi.org/10.1016/j.wse.2021.08.003
25. Puari, A., Rusnam, R., Yanti, N. R., Shukor, M. Y. (2024). Innuence of carbonization process parameters on copper (II) ion adsorption performance of biochar from exhausted coffee husk (ECH). *IOP Conference Series: Earth and Environmental Science*. https://doi.org/10.1088/1755-1315/1426/1/012011
26. Puari, A. T., Azora, A., Rusnam, R., Yanti, N. R. (2024). Biosorption optimization and mechanism of biochar from exhausted coffee husk on iron in aqueous solution using response surface methodology. *Case Studies in Chemical and Environmental Engineering*, *10*(April), 100816. https://doi.org/10.1016/j.cscee.2024.100816
27. Puari, A. T., Azora, A., Rusnam, R., Yanti, N. R., Arlius, F., Shukor, M. Y. (2024a). Carbonization parameters optimization for the biosorption capacity of Cu2+ by a novel biosorbent from agroindustrial solid waste using response surface methodology. *Case Studies in Chemical and Environmental Engineering*, *9*(January), 100645. https://doi.org/10.1016/j.cscee.2024.100645
28. Puari, A. T., Azora, A., Rusnam, R., Yanti, N. R., Arlius, F., Shukor, M. Y. (2024b). Carbonization parameters optimization for the biosorption capacity of Cu2+ by a novel biosorbent from agroindustrial solid waste using response surface methodology. *Case Studies in Chemical and Environmental Engineering*, *9*, 100645. https://doi.org/10.1016/j.cscee.2024.100645
29. Puari, A. T., Yanti, N. R., Sari, N., Rusnam, R. (2024). Response surface methodology (RSM) for optimization carbonization parameters of exhausted coffee husk for iron removal from aqueous solution. *Jurnal Teknik Pertanian Lampung (Journal of Agricultural Engineering)*, *13*(3), 637. https://doi.org/10.23960/jtep-l.v13i3.637-649
30. Puari, A. T., Anandika, A., Apriani, I. I., Azora, A., Maida, S. P. (2025). Contamination level of heavy metals and assessment of the ecologic risk in the surface water and sediments of Batanghari river, Dharmasraya region, Indonesia. *Journal of Ecological Engineering*, *26*(4), 182–197.
31. Puari, R., R., Yanti, N. R. (2022). Optimization of the carbonization parameter of exhausted coffee husk (ECH) as biochar for Pb and Cu removal based on energy consumption. *Jurnal Teknik Pertanian Lampung*, *11*(2). https://doi.org/10.23960/jtep-l.v11.i2.242-252
32. Rashid, R., Shafiq, I., Akhter, P., Iqbal, M. J., Hussain, M. (2021). A state-of-the-art review on wastewater treatment techniques: the effectiveness of adsorption method. *Environmental Science and Pollution Research 2021 28:8*, *28*(8), 9050–9066. https://doi.org/10.1007/S11356-021-12395-X
33. Rusnam, R., Puari, A. T., Yanti, N. R., Efrizal, E. (2022). Utilisation of exhausted coffee husk as low-cost bio-sorbent for adsorption of Pb2+. *Tropical Life Science Research*, *33*(3), 229–252. https://doi.org/https://doi.org/10.21315/tlsr2022.33.3.12
34. Sagar J. P., Pradhan, A., Prakash N. S., Kishore D. A., Naik, B. (2022). Biosorption of heavy metals from wastewater using Saccharomyces cerevisiae as a biosorbent: A mini review. *Materials Today: Proceedings*, *67*, 1140–1146. https://doi.org/10.1016/j.matpr.2022.07.306
35. Satyam, S., Patra, S. (2024). Innovations and challenges in adsorption-based wastewater remediation: A comprehensive review. *Heliyon*, *10*(9), e29573. https://doi.org/10.1016/j.heliyon.2024.e29573
36. Semerjian, L. (2018). Removal of heavy metals (Cu, Pb) from aqueous solutions using pine (*Pinus halepensis*) sawdust: Equilibrium, kinetic, and thermodynamic studies. *Environmental Technology and Innovation*, *12*, 91–103. https://doi.org/10.1016/j.eti.2018.08.005
37. Tian, S., Gong, X., Yu, Q., Yao, F., Li, W., Guo, Z., Zhang, X., Yuan, Y., Fan, Y., Bian, R., Wang, Y., Zhang, X., Li, L., Pan, G. (2023). Efficient removal

of Cd(II) and Pb(II) from aqueous solution using biochars derived from food waste. *Environmental Science and Pollution Research International*, *30*(58), 122364–122380. https://doi.org/10.1007/s11356-023-30777-1

38. Wang, L., Gao, H., Wang, M., Xue, J. (2022). Remediation of petroleum-contaminated soil by ball milling and reuse as heavy metal adsorbent. *Journal of Hazardous Materials*, *424*, 127305. https://doi.org/10.1016/J.JHAZMAT.2021.127305
39. Wang, Q., Wang, Y., Yang, Z., Han, W., Yuan, L., Zhang, L., Huang, X. (2022). Efficient removal of Pb(II) and Cd(II) from aqueous solutions by mango seed biosorbent. *Chemical Engineering Journal Advances*, *11*(March), 100295. https://doi.org/10.1016/j.ceja.2022.100295
40. Wang, X., Wang, X., Chen, W., Yuan, J., Zhang, Q. (2025). Adsorption of Cu(II) and Pb(II) in aqueous solution by biochar composites. *ACS Omega*, *Ii*. https://doi.org/10.1021/acsomega.4c06837
41. Yang, X., Cui, X. (2013). Adsorption characteristics of Pb (II) on alkali treated tea residue. *Water Resources and Industry*, *3*, 1–10. https://doi.org/10.1016/j.wri.2013.05.003
42. Zhang, Y., Li, A., Liu, L., Duan, X., Ge, W., Liu, C., Qiu, G. (2023). Enhanced remediation of cadmium-polluted soil and water using facilely prepared MnO_2-coated rice husk biomass. *Chemical Engineering Journal*, *457*, 141311. https://doi.org/10.1016/J.CEJ.2023.141311
43. Zhou, R., Zhang, M., Zhou, J., Wang, J. (2019). Optimization of biochar preparation from the stem of Eichhornia crassipes using response surface methodology on adsorption of Cd2+. *Scientific Reports*, *9*(1), 1–17. https://doi.org/10.1038/s41598-019-54105-1